JOURNAL OF Materials CHEMISTRY

# Metal-rich mixed chalcogenides $TaNi_2Q_2$ (Q = Se,Te): synthesis, structure and electronic properties

**Vladimir K. Evstafiev, Jörg Neuhausen, E. Wolfgang Finckh and Wolfgang Tremel*†**

*Institut für Anorganische Chemie und Analytische Chemie der Johannes Gutenberg-Universität, J.-J.-Becherweg 24, D-55099 Mainz, Germany*

Phases in the pseudo-binary system $TaNi_2Se_xTe_{2-x}$ ($0 \leqslant x \leqslant 1$) have been prepared by high temperature methods. According to the results of powder X-ray diffraction all phases crystallize isotypic to $TaNi_2Te_2$ in the orthorhombic space group *Pnma* (no. 62). The lattice parameters in the $TaNi_2Se_xTe_{2-x}$ system show a complex behaviour as a function of composition. The structure of $TaNi_2SeTe$ was determined by single crystal methods. $TaNi_2SeTe$ is built up from $TaNi_2$-layers which are sandwiched by chalcogen sheets. The chalcogen atoms are ordered on two independent crystallographic postitions. In agreement with size considerations the Se atoms have four metal neighbours while the Te atoms have five neighboring metal atoms. We have not been able to achieve a substitution by Se on the Te site with five metal neighbours so far. $TaNi_2SeTe$ is metallic and shows Pauli paramagnetic behaviour, as expected from the results of TB-LMTO-ASA band structure calculations.

## Introduction

Transition metal chalcogenides have been of interest in chemistry and materials science because of their outstanding physical and chemical properties such as charge density wave behaviour,[1–4] superconductivity,[5,6] intercalation reactions[7–9] and surface modification by scanning probe microscopy techniques.[10,11] In the last years a large number of binary and ternary tellurides such as $Ta_2Te_3$,[12,13] $M_3M'Te_6$ (M = Nb, Ta; M′ = Si, Ge),[14–17] $M_4M'Te_4$ (M = Nb, Ta; M′ = Si, Cr, Fe, Co),[18–20] $MGeTe_4$ (M = Zr, Hf)[21] and.$Ta_{1.09}Fe_{2.39}Te_4$[22] have been synthesized and characterized. Many of them are chemically unique in the sense that there is no Se-analogue. The reason for this behaviour is not yet understood based either on chemical reasoning or on electronic structure calculations. Among these new telluride materials the metal rich (metal to chalcogen ratio $\geqslant 1$) ternary Nb,Ta tellurides with a late transition metal (Fe, Co, Ni) as the third constituent, *e.g.* $MM'Te_2$ (M = Nb, Ta; M′ = Fe, Co, Ni)[23–27] or $MNi_{2+x}Te_3$ (M = Nb, Ta)[28,29] are a particularly interesting class of compounds. These compounds form layered structures containing metal clusters which can be connected in various different fashions. Many of these phases have interesting properties such as magnetic transitions in $TaFe_{1+x}Te_3$[30] or electronically driven structural transformations in $TaM'_2Te_2$ (M = Co, Ni).[25,31] Recently, we discovered the first example of a Se-analogue for a representative of this class, *i.e.* $Ta_2Ni_3Se_5$.[32] Motivated by this, we have undertaken a systematic study of Se-substitution in these systems. In this paper we report the results obtained on the system $TaNi_2(Se,Te)_2$.

## Experimental

### Synthesis

Samples in the system $TaNi_2Se_xTe_{2-x}$ ($0 \leqslant x \leqslant 1$) were prepared from stoichiometric mixtures of the elements: Ta powder (Starck, 99.8%), Ni powder (Alfa, 99.9%), Se powder (Merck, 99.9%) and Te powder (Merck, 99.9%). The samples were heated at 900 °C for 6 days in previously outgassed quartz tubes (length *ca.* 4 cm, diameter 12 mm) sealed under vacuum (*ca.* $10^{-3}$ Pa). For the solid solution series $TaNi_2Se_xTe_{2-x}$ the parameter $x$ was varied in steps of 0.1. According to the results of X-ray Guinier photographs the samples contain small amounts of $Ta_2O_5$[33] and Ni(Se,Te).[34–39] Since these impurities are present only in very small amounts, the sample composition is assumed to be identical to the starting composition. The composition was also checked by energy-dispersive X-ray analysis (EDX) in a scanning electron microscope (Zeiss DSM 962) and has been found to correspond to the nominal composition within the experimental error. Single crystals of $TaNi_2SeTe$ were grown in longer tubes (10 cm) using a small amount (*ca.* 15 mg) of iodine as a mineralizer. Attempts to prepare samples with $x \geqslant 1$ led to the formation of a second phase of $TaNi_ySe_2$-type[40,41] and an increasing amount of the above mentioned impurities.

### Crystallographic studies

**X-Ray powder diffraction.** Samples in the system $TaNi_2Se_xTe_{2-x}$ ($0 \leqslant x \leqslant 1$) were characterized using a Philips PW 1840 powder diffractometer [Bragg–Brentano geometry, Ni-filtered CuKα-radiation ($\lambda = 1.5418$ Å), Si-solid state detector]. The obtained powder patterns could be indexed based on the powder pattern of $TaNi_2Te_2$[31] calculated using the program LAZY-PULVERIX.[42] The measured reflection profiles were fitted using a pseudo-Voigt function (program PROFAN[43]). The obtained peak positions were used to refine lattice parameters employing a least squares procedure (program LATTIC[43]).

**Single crystal X-ray studies.** For single crystal structure determination a plate-like shaped crystal of $TaNi_2SeTe$ (approximate dimensions $0.35 \times 0.15 \times 0.025$ mm) was mounted on an automated Syntex $P2_1$ four-circle diffractometer equipped with a graphite monochromator and a scintillation counter using MoKα-radiation ($\lambda = 0.710\,73$ Å).

Lattice constants were determined from the angular positions of 25 carefully centered reflections with $15° \leqslant 2\theta \leqslant 30°$. Two octants ($+h, \pm k, +l$) were measured in an angular range of $4° \leqslant 2\theta \leqslant 60°$ using the $\theta$–$2\theta$ technique. The intensities of three standard reflections were scanned after every 97 reflections indicating no decomposition of the sample. Lorentz and polarisation corrections as well as a semi-empirical absorption correction ($\psi$-scan) were applied to the data.

The systematic extinctions are in accordance with the space groups *Pnma* (no. 62) and $Pna2_1$ (no. 33). The distribution of normalized structure factors suggested the presence of a center

†e-mail: tremel@indigotrem1.chemie.uni-mainz.de

of symmetry. The structure was solved and refined in the centrosymmetric space group *Pnma*. Refinements in the non-centrosymmetric space group $Pna2_1$ resulted in strong correlations of parameters due to the presence of a center of symmetry in the structure.

Direct methods (SHELXS[44]) yielded a starting structural model consisting of one Ta, two Ni and two chalcogen atoms very similar to the known structure of $TaNi_2Te_2$.[31] The electron densities of the two chalcogen sites were very different, suggesting an ordering of the chalcogen atoms. Therefore, the site with lower electron density was assumed to be occupied by Se, whereas the site with higher electron density was assigned to Te. This ordering was verified by the successful refinement. A statistical occupation of the chalcogen sites by both sorts of atoms can be clearly ruled out. The final refinements employing anisotropic thermal parameters and an extinction correction resulted in residual values of $R=0.041$ and $R_w=0.042$. Details of the structure determination are summarized in Table 1. Final positional parameters, equivalent isotropic thermal parameters and important interatomic distances are listed in Tables 2 and 3.

Full crystallographic details, excluding structure factors, have been deposited at the Cambridge Crystallographic Data Centre (CCDC). See Information for Authors, *J. Mater. Chem.*, 1998, Issue 1. Any request to the CCDC for this material should quote the full literature citation and the reference number 1145/101.

### Resistivity measurements

Resistivity measurements were performed using a four point method standard in this laboratory. Details concerning the experimental setup are given in ref. 45. A plate-like shaped crystal of $TaNi_2SeTe$ (dimensions *ca.* $3\times1.5\times0.5$ mm) was glued to a glass slide. The glass slide was mounted on a sample holder and four gold wires were attached to the corners of the plate-like crystal using silver epoxy glue. The conductivity was measured from 5 to 295 K in steps of 2 K both on heating and cooling.

**Table 1** Crystal data for $TaNi_2SeTe$

| | |
|---|---|
| formula | $TaNi_2SeTe$ |
| formula mass/g mol$^{-1}$ | 504.9 |
| crystal system | orthorhombic |
| space group | *Pnma* (no. 62) |
| lattice parameters/Å | $a=6.528(1)$ |
| | $b=3.504(1)$ |
| | $c=16.478(3)$ |
| unit cell volume/Å$^3$ | 376.9(1) |
| formula units per cell | 4 |
| temperature of data collection/K | 298 |
| crystal shape | rectangular plate |
| crystal dimensions/mm | $0.35\times0.15\times0.025$ |
| calculated density/g cm$^{-3}$ | 8.898 |
| diffractometer | Syntex $P2_1$ |
| radiation | MoKα ($\lambda=0.710\,73$ Å) |
| linear absorption coefficient/mm$^{-1}$ | 55.832 |
| monochromator | graphite, parallel |
| measured $2\theta$-range/° | 4–60 |
| scan type | $\theta$-$2\theta$ |
| scan range | 1.8° + Kα-splitting |
| scan speed/° min$^{-1}$ | variable, 2.55–29.3 |
| measured octants | $+h,\ \pm k,\ +l$ |
| measured reflections | 1021 |
| unique reflections | 618 |
| $R_{int}$ | 0.036 |
| observed reflections [$I>2\sigma(I)$] | 580 |
| absorption correction | semi-empirical, $\psi$-Scan, 2 reflections |
| minimum (maximum) transmission | 0.2834 (0.7871) |
| structure solution | direct methods |
| structure refinement | full matrix least squares |
| minimized quantity | $\Sigma w(F_o-F_c)^2$ |
| number of parameters | 32 |
| weighting scheme | $w=1/[\sigma^2(F_o)+0.00005F_o^2]$ |
| extinction correction[a] | 0.0039(2) |
| $R(R_w)$[b] | 0.041(0.042) |
| goodness of fit (GOF)[c] | 1.36 |
| difference fourier maximum/e Å$^{-3}$ | 3.96 |

[a] $F_c^{cor}=F_c[1+0.0002\chi F^2{}_c/\sin(2\theta)]^{-1/4}$. [b] $R=\Sigma||F_o|-|F_c||/\Sigma|F_o|$, $R_w=[\Sigma w'||F_o|-|F_c||^2/\Sigma w|F_o|^2]^{1/2}$. [c] $GOF=[\Sigma w||F_o|-|F_c||^2/(m-n)]^{1/2}$, where $m$ and $n$ are the numbers of data and parameters, respectively.

**Table 2** Positional parameters and equivalent isotropic thermal parameters ($U_{eq}$)[a] for $TaNi_2SeTe$

| Atom | site | $x/a$ | $y/b$ | $z/c$ | $U_{eq}$/Å$^2$ |
|---|---|---|---|---|---|
| Ta | 4c | 0.90603(7) | 1/4 | 0.27821(3) | 0.0076(2) |
| Ni(1) | 4c | 0.6034(2) | 3/4 | 0.3198(1) | 0.0093(4) |
| Ni(2) | 4c | 0.7159(2) | 3/4 | 0.1793(1) | 0.0097(4) |
| Te | 4c | 0.9103(1) | 1/4 | 0.09762(5) | 0.0128(3) |
| Se | 4c | 0.9092(2) | 3/4 | 0.40318(8) | 0.0094(4) |

[a] Equivalent isotropic $U$ is defined as one third of the trace of the orthogonalized $U_{ij}$ tensor.

**Table 3** Important interatomic distances (Å) for $TaNi_2SeTe$

| | | | |
|---|---|---|---|
| Ta—Ni(1) | 2.705(1) (2×) | Ta—Te | 2.976(1) |
| Ta—Ni(1) | 2.752(1) (2×) | Ta—Se | 2.704(1) (2×) |
| Ta—Ni(2) | 2.699(1) (2×) | | |
| Ta—Ni(2) | 2.742(1) (2×) | Ta—Ta | 3.504(1) (2×) |
| | | Ta—Ta | 3.394(1) (2×) |
| Ni(1)—Te | 2.548(1) (2×) | | |
| Ni(1)—Se | 2.420(2) | Ni(1)—Ni(2) | 2.428(2) |
| Ni(2)—Te | 2.552(2) (2×) | Ni(1)—Ni(2) | 2.530(2) |
| Ni(2)—Se | 2.424(2) | | |
| Q—Q distances within the layer: | | | |
| Te—Te | 3.504(1) (2×) | Se—Se | 3.504(1) (2×) |
| Te—Se | 3.698(2) (2×) | Se—Se | 3.698(2) (2×) |
| Te—Se | 3.711(2) (2×) | Se—Se | 3.711(2) (2×) |
| Q—Q distances betweeen the layers: | | | |
| Te—Te | 3.846(2) (2×) | Se—Te | 3.823(2) |
| Te—Se | 3.823(2) | Se—Se | 3.828(3) (2×) |

### Electronic structure calculations

The electronic structure of $TaNi_2SeTe$ was determined by first principles methods. Band structure calculations were performed based on the structural parameters given in Table 2 using the TB-LMTO-ASA program package.[46–48]

## Results and Discussion

### The structure of $TaNi_2SeTe$

The structure of $TaNi_2SeTe$ can be derived from the $TaNi_2Te_2$ structure[31] by substitution of one of the two crystallographically independent Te atoms by Se. The structure is built up from layers of composition $TaNi_2SeTe$, which are stacked along the crystallographic $c$ direction. There are two of these layers per unit cell, which are related by an $n$-glide. The shortest chalcogen–chalcogen distances between the layers are $d_{Te—Te}=3.846(2)$ Å, $d_{Se—Te}=3.823(2)$ Å and $d_{Se—Se}=3.828(3)$ Å. Therefore, only weak van der Waals interactions exist between the layers. This is also reflected by the fact that the crystals can be cleaved easily. Within the layers, there are chalcogen–chalcogen distances as short as 3.504(1) Å. Significant interactions have to be considered for the corresponding Te—Te contacts. On the other hand, the corresponding Se—Se distances are slightly longer than the non-bonding contacts in trigonal Se ($d_{Se—Se}=3.44$ Å)[49] or in metal-rich selenides such as $Nb_2Se$ and $Nb_5Se_4$ ($d_{Se—Se}=3.42$–$3.45$ Å).[50]

Fig. 1 shows a perspective representation of the structure projected along the crystallographic $b$ direction. A projection of a single $TaNi_2SeTe$ slab is shown in Fig. 2. A simple description of the $TaNi_2SeTe$ structure starts from a *cis–trans* chain of Ni atoms running parallel to the crystallographic *a*

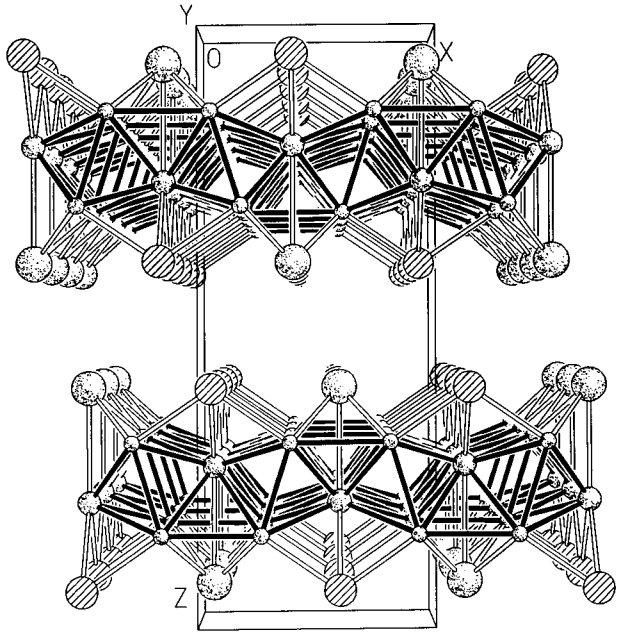


**Fig. 1** Perspective view of the $TaNi_2SeTe$ structure along [010]; large dotted circles: Te; large hatched circles: Se; medium dotted circles: Ta; small dotted circles: Ni

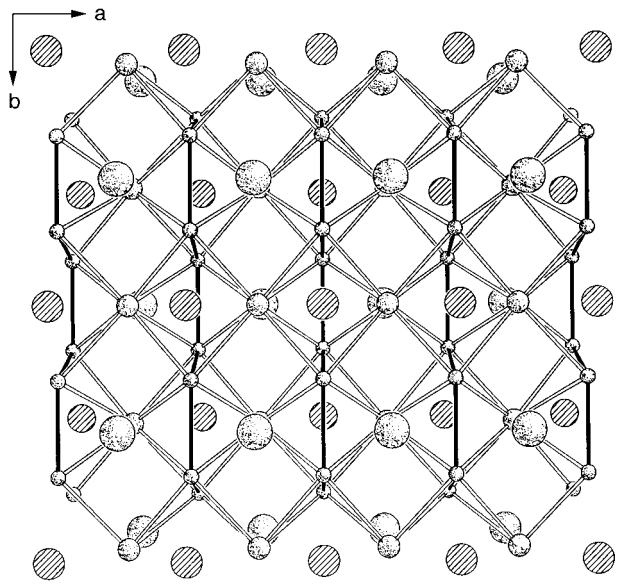


**Fig. 2** Projection of a single $TaNi_2SeTe$ layer along [001]; large dotted circles: Te; large hatched circles: Se; medium dotted circles: Ta; small dotted circles: Ni

axis. The Ni—Ni distances within the chain are 2.428(2) and 2.530(2) Å very similar to the end-member $TaNi_2Te_2$ [2.407(2) and 2.524(2) Å]. These distances are also comparable to those in Ni metal[51] and related compounds such as $TaNiTe_2$ and $Ta_2Ni_3Te_5$.[24] The *cis–trans* Ni chains are connected by Ta atoms which are attached to six Ni—Ni bonds in a side-on fashion. Thereby each Ta atom has eight Ni neighbours, each Ni atom four Ta and two Ni neighbours, the average Ta—Ni distance being 2.725 Å ($TaNi_2Te_2$: 2.733 Å[31]). The Ta—Ta separations along the crystallographic *a* direction are 3.394(1) Å [$TaNi_2Te_2$: 3.370(1) Å[31]]. The Ta—Ta distances along the *b* direction correspond to the lattice constant *b* [$TaNi_2SeTe$: 3.504(1) Å; $TaNi_2Te_2$: 3.566(1) Å[31]]. The Se and Te atoms are situated in fourfold $\mu_4$ and fivefold $\mu_5$ bridging positions above and below the $TaNi_2$ slab, respectively. The $\mu_4$-Se atom is connected to two Ni and two Ta atoms, whereas the $\mu_5$-Te atom is bonded to four Ni atoms and one Ta atom.

An alternative description starts by considering a square net of $Ni_2$ dumbbells in a plane parallel and the Ni—Ni vector perpendicular to the crystallographic *ab* plane. The Ni—Ni distance within the dumbbells is 2.428(2) Å, the distance between the dumbbells is *ca.* 3.5 Å. A 18° and −18° tilt of the $Ni_2$ dumbbells with respect to an axis parallel to *b* leads to alternating Ni—Ni distances of 2.530(2) and 3.952(2) Å. The resulting distorted square $Ni_2$ net is interpenetrated by an idealized square-planar net of Ta atoms, the Ta—Ta separations being 3.504(1) and 3.394(1) Å. This $TaNi_2$ slab is capped from above and below by chalcogen atoms.

Naturally, the main structural differences between $TaNi_2SeTe$ and $TaNi_2Te_2$ arise from the substitution of one of the Te atoms, *i.e.* the $\mu_4$-Te, by Se. Attempts to substitute the $\mu_5$-Te atom by Se have not been successful so far. This is in agreement with the size of the chalcogen atoms. The smaller Se atoms prefer to be bonded to four metal atoms, whereas the large Te atoms are connected to five metal atoms.

The ordered substitution of Te by Se results in the occurrence of rows of chalcogen atoms which exclusively consist of either Se or Te and run parallel to the crystallographic *b* direction. These rows alternate along the crystallographic *a* direction. The chalcogen–chalcogen distances within these rows are 3.504(1) Å. Thus, they are the closest chalcogen–chalcogen contacts in this structure. The value of 3.504(1) Å can be considered as non-bonding for the Se—Se contacts, whereas significant interactions have to be considered for the corresponding Te—Te distances. Similar distances occur in all members of the $TaM'_2Se_xTe_{2-x}$ family (M′=Ni, Co; $x \leqslant 1$).[25,31,52,53] The remaining chalcogen–chalcogen distances range between 3.698 and 3.846 Å (see Table 3 for details). Te—Te distances in this regime are typical for non-bonding contacts in strongly covalent compounds such as $TaNiTe_2$ ($d_{Te-Te} \geqslant 3.846$ Å)[24] or $TaNi_{2.05}Te_3$ ($d_{Te-Te} \geqslant 3.701$ Å).[28] The corresponding Se—Te and Se—Se distances have to considered as unusually long. Typical Se—Se distances in covalent compounds are considerably shorter (*e.g.* $d_{Se-Se} = 3.45$ Å in $Nb_5Se_4$[50]). Therefore, the chalcogen sheets in the $TaNi_2SeTe$ structure cannnot be considered as close packed. This may be one reason why a complete substitution of Te by Se is not possible.

### The solid solution series $TaNi_2Se_xTe_{2-x}$

The lattice parameters for the system $TaNi_2Se_xTe_{2-x}$, as derived from powder X-ray diffraction, are plotted *vs.* the composition *x* in Fig. 3. The lattice parameters vary smoothly with changing composition without any discontinuities, implying a solid solution series in the region $0 \leqslant x \leqslant 1$. Comparing the behaviour of the different lattice parameters, one observes that the largest change occurs in the *c* parameter wich runs parallel to the stacking directions of the layers. This parameter decreases smoothly as *x* increases throughout the complete solid solution range. The *b* parameter also shows a smooth, almost linear decrease with increasing *x*, although here the changes are much smaller. In contrast, the *a* parameter increases slightly as *x* increases, running through a plateau in the region $0.2 \leqslant x \leqslant 0.7$. The resulting cell volume shows a smooth decrease with increasing Se content.

This behaviour can be understood considering that metal–metal interactions play an important role in the chemical bonding *within* the layers. In the stacking direction of the layers a large compression of the corresponding lattice parameter *c* can occur when substituting Te by the smaller Se atoms. van der Waals interactions are predominant in the interlayer region. Therefore, the interlayer distances are determined by the van der Waals radii of the chalcogen atoms. On the other hand the 'thickness' of the layers is dependent mainly on the

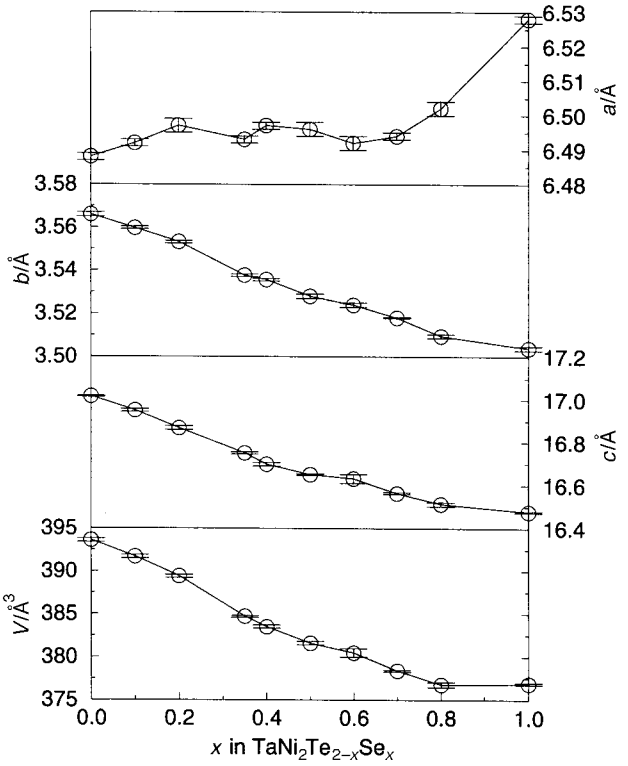


**Fig. 3** Lattice parameters for the phases in the system $TaNi_2Se_xTe_{2-x}$ plotted *vs.* composition

metal–chalcogen distances. Both values decrease with decreasing average chalcogen atom size. Within the layers a compression of the lattice would lead to a shortening of both metal–chalcogen and metal–metal distances. The former would be favorable when substituting Te by Se. This is overcompensated by an increase of metal–metal antibonding interactions, which would be caused by a compression of the metal sublattice.

## Electronic properties

Similar to the parent compound $TaNi_2Te_2$, the phases in the system $TaNi_2Se_xTe_{2-x}$ show simple metallic and Pauli paramagnetic behaviour. A plot of the resistivity *vs.* temperature for $TaNi_2SeTe$ is shown in Fig. 4. This was expected from the results of TB-LMTO-ASA band structure calculations. Fig. 5 shows the density of states (DOS) calculated for $TaNi_2SeTe$. At the Fermi level there is a significant DOS giving rise to metallic conductivity. The majority of the states around the

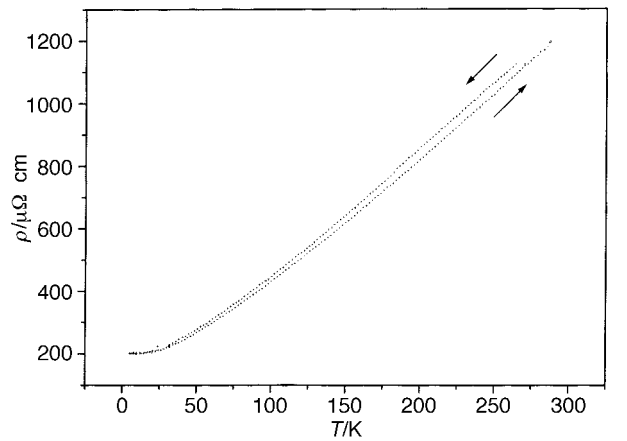


**Fig. 4** Plot of the resistivity of $TaNi_2SeTe$ *vs.* temperature. Cooling and heating cycles are shown

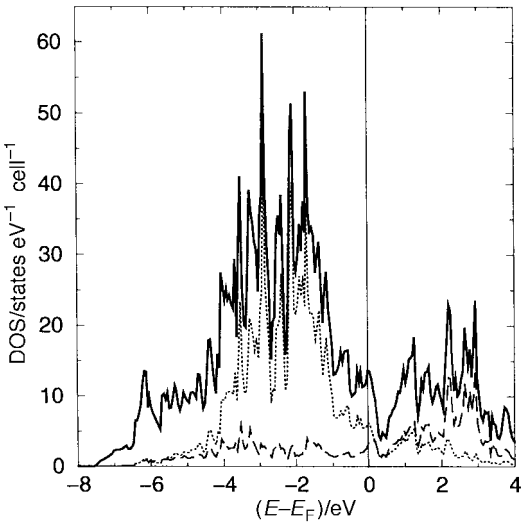


**Fig. 5** Density of states calculated using the LMTO method. The Fermi level is marked by a vertical bar; solid line: total DOS; dotted line: Ni d states; dashed line: Ta d states

Fermi level is metal centered. States with mostly chalcogen character are located in the low energy region (not depicted here) as expected from the relatively high electronegativity of the chalcogens. Due to the relatively contracted 3d orbitals of Ni the corresponding states are located in a fairly small energy interval giving rise to a pronounced peak in the DOS slightly below the Fermi level. The Ta 5d orbitals are more diffuse. Therefore the corresponding states cover a wide region around the Fermi level ranging from −5 to 4 eV with a maximum around 2–3 eV.

## References


1 J. A. Wilson, F. J. DiSalvo and S. Mahajan, *Adv. Phys.,* 1975, **24**, 117.
2 *Crystal Chemistry and Properties of Materials with Quasi One-Dimensional Structures*, ed. J. Rouxel, Reidel, Dordrecht, 1986.
3 *Electronic Properties of Inorganic Quasi One-Dimensional Compounds*, Part 1 and 2, ed. P. Monceau, Reidel, Dordrecht, 1985.
4 *Theoretical Aspects of Band Structures and Electronic Properties of Pseudo One-Dimensional Solids*, ed. H. Kamimura, Reidel, Dordrecht, 1985.
5 K. Yvon, *Curr. Top. Mater. Sci.,* 1979, **3**, 53.
6 R. Chevrel, in *Superconductor Materials Science*, ed. S. Flomer and B. B. Schwartz, Plenum, New York, 1981, ch. 10.
7 *Intercalation Chemistry*, ed. M. S. Wittingham and A. J. Jacobsen, Academic Press, New York, 1982.
8 R. H. Friend and A. D. Yoffe, *Adv. Phys.*, 1987, **36**, 1.
9 J. Rouxel and R. Brec, *Annu. Rev. Mater. Sci.*, 1986, **16**, 137.
10 H. Fuchs and T. Schimmel, *Adv. Mater.*, 1991, **3**, 112.
11 H. Fuchs, R. Laschinski and T. Schimmel, *Europhys. Lett.,* 1990, **13**, 307.
12 M. Conrad and B. Harbrecht, *J. Alloys Compd.,* 1992, **187**, 181.
13 H. Kleinke, Diploma Thesis, University of Münster, 1991.
14 L. Monconduit, M. Evain, F. Boucher, R. Brec and J. Rouxel, *Z. Anorg. Allg. Chem.,* 1992, **616**, 177.
15 E. Canadell, L. Monconduit, M. Evain, R. Brec, J. Rouxel and M.-H. Whangbo, *Inorg. Chem.,* 1993, **32**, 10.
16 J. Li and P. J. Caroll, *Mater. Res. Bull.,* 1992, **27**, 1073; J. Li, M. E. Badding and F. J. DiSalvo, *J. Alloys Compd.,* 1993, **184**, 257.
17 W. Tremel, H. Kleinke, V. Derstroff and C. Reisner, *J. Alloys Compd.*, 1995, **219**, 73.
18 M. E. Badding and F. J. DiSalvo, *Inorg. Chem.*, 1990, **29**, 3952.
19 K. Ahn, T. Hughbanks, K. D. D. Rathnayaka and D. G. Naugle, *Chem. Mater.*, 1994, **6**, 418.
20 J. Neuhausen, E. W. Finckh and W. Tremel, *Chem Ber.*, 1995, **128**, 569.
21 A. Mar and J. A. Ibers, *J. Am. Chem. Soc.*, 1993, **115**, 3227.
22 J. Neuhausen and W. Tremel, *J. Alloys Compd.*, 1994, **204**, 215.
23 J. L. Huang, S. X. Liu and B. Q. Huang, *Sci. China, Ser. B*, 1991, **34**, 666.

24 W. Tremel, *Angew. Chem*., 1991, **103**, 900; *Angew. Chem., Int. Ed. Engl*., 1991, **30**, 840.
25 W. Tremel, *J. Chem Soc., Chem. Commun*., 1991, 1405.
26 J. Neuhausen, K.-L. Stork, E. Potthoff and W. Tremel, *Z. Naturforsch., Teil B*, 1992, **47**, 1203.
27 J. Li, M. E. Badding and F. J. DiSalvo, *Inorg. Chem*., 1992, **31**, 1050.
28 J. Neuhausen, V. K. Evstafyev, R. K. Kremer and W. Tremel, *Chem. Ber*., 1994, **127**, 1621.
29 J. Neuhausen, E. W. Finckh and W. Tremel, *Inorg. Chem*., 1995, **34**, 3823.
30 J. Neuhausen, E. Potthoff, W. Tremel, J. Ensling and P. Gütlich, *Z. Naturforsch., Teil B*, 1993, **48**, 797.
31 W. Tremel, *Angew. Chem*., 1992, **104**, 230; *Angew. Chem*., *Int. Ed. Engl*., 1992, **231**, 217.
32 J. Neuhausen and W. Tremel, *Proceedings: Soft chemistry Routes to New Materials*, Trans Tech Publications, Aedermannsdorf, vol. 152–153, p. 383.
33 K. Lehovec, *J. Less-Common Met*., 1964, **7**, 397.
34 E. Røst and E. Vestersjø, *Acta Chem. Scand*., 1968, **22**, 2118.
35 S. Furuseth, A. Kjekshus and A. F. Andersen, *Acta Chem. Scand*., 1969, **23**, 2325.
36 K. Haugsten and E. Røst, *Acta Chem. Scand,* 1972, **26**, 410.
37 F. Grønvold, *Acta Chem. Scand*., 1970, **24**, 1036.
38 K. L. Komarek and K. Wessely, *Monatsh. Chem*., 1972, **103**, 896.
39 F. Bøhm, F. Grønvold, H. Haraldsen and H. Prydz, *Acta Chem. Scand*., 1955, **9**, 1510.
40 J. M. van den Berg and P. Cossee, *Inorg. Chim. Acta*, 1968, **2**, 143.
41 A. R. Beal, in *Physics and Chemistry of Materials with Layerd Structures*, ed. F. Lévy, Reidel, Dordrecht, 1979, vol. 6.
42 K. Yvon, W. Jeitschko and E. Parthé, *J. Appl. Crystallogr*., 1977, **10**, 73.
43 L. G. Akselrud and V. K. Percharsky, *CSD program package*, L′viv, 1991.
44 *SHELXTL-Plus program package*, Siemens Analytical X-Ray Instruments, Madison, WI, 1991.
45 H. Kleinke, E. W. Finckh and W. Tremel, *Z. Anorg. Allg. Chem*., in press.
46 G. Krier, O. Jepsen, A. Burkhardt and O. K. Andersen, Program TB-LMTO-ASA 4.7 (tight binding-linear muffin tin orbital-atomic sphere approximation), Stuttgart, 1996.
47 O. K. Andersen, *Phys. Rev. B* 1975, **12**, 3060.
48 O. K. Andersen and O. Jepsen, *Phys. Rev. Lett*., 1984, **53**, 2571.
49 P. Cherin and P. Unger, *Inorg. Chem*., 1967, **6**, 1589.
50 H. F. Franzen, *Prog. Solid State Chem*., 1978, **12**, 1.
51 A. F. Holleman and E. Wiberg, *Lehrbuch der Anorganischen Chemie*, Walter de Gruyter, Berlin, 1985.
52 J. Neuhausen, V. K. Evstaf'iev, T. Block, E. W. Finckh, W. Tremel, L. Augustin, H. Fuchs, D. Voß, P. Krüger, A. Mazur and J. Pollmann, *Chem. Mater*., in press.
53 J. Neuhausen, V. K. Evstaf'iev, E. W. Finckh, W. Tremel, L. Augustin and H. Fuchs, to be published.

*Paper* 8/02216J; *Received* 20*th March*, 1998